



JNK3 quantification in plasma: a novel biomarker for neuronal damage in Parkinson's disease



Elena Vacchi^{1,2,15}, Arianna Giani^{3,4,15}, Nunzio Perta^{4,5}, Sara Turchetti^{3,4}, Laura Pasetto⁴, Valentina Bonetto⁴, Maria Giulia Bacalini⁶, Luca Baldelli^{6,7}, Federica Provini^{6,7}, Sandra Hackethal⁸, Silvia Riccardi⁸, Silvia Miano^{2,8}, Mauro Manconi^{2,8}, Georg Kägi^{9,10}, Ilaria Bertaina¹¹, Giovanni Bianco¹¹, Salvatore Galati^{2,11}, Alain Kaelin-Lang^{2,11}, Domenico Raimondo¹², Mariaelena Repici¹³, Mauro Tettamanti¹⁴, Giorgia Melli^{1,2,11}✉ & Tiziana Borsello^{3,4}✉

Diagnosis of Parkinson's disease (PD) remains challenging due to the lack of reliable biomarkers. To address this need, we quantified plasma levels of brain-specific c-Jun N-terminal kinase 3 (JNK3), a protein involved in neurodegeneration. A total of 108 participants were enrolled, including 25 individuals with isolated REM sleep behavior disorder (iRBD), 26 patients with De Novo PD, 29 with Late PD, and 28 age-matched healthy controls (HC). All subjects underwent clinical assessment, blood sampling, and skin biopsy. Plasma JNK3 levels were significantly elevated in PD and iRBD compared to HC, a finding that remained robust after adjustment for age and sex in multivariate logistic regression. ROC analysis demonstrated that JNK3 levels distinguished PD from HC with 100% specificity and 65% sensitivity in Late PD. In contrast, Neurofilament Light Chain showed non-significant group differences and weak discriminative performance. Notably, while JNK3 declined with age in HC, it increased with age in Late PD ($P = 0.048$, $B = 0.105$) and negatively correlated with motor impairment. Elevated JNK3 was also associated with pathological α -Synuclein in skin biopsy. These findings highlight JNK3 as a promising blood biomarker for PD, with meaningful diagnostic and prognostic value, suggesting that its implementation could refine patient stratification and improve clinical trial efficiency.

Parkinson's disease (PD) is one of the most prevalent neurodegenerative disorders, with its incidence rapidly increasing worldwide¹. The progression of PD often spans several years, and its clinical presentation is marked by considerable heterogeneity in both symptoms and disease trajectory among individuals². Recently, the underlying biology of PD has been categorized in

terms of three key pathological processes: presence or absence of synucleinopathy, evidence of neurodegeneration, and identification of genetic factors^{3,4}. In most cases, PD is characterized by the pathological aggregation of α -Synuclein (α -Syn) in both the central and peripheral nervous systems, with emerging evidence suggesting that the propagation of these aggregates

¹Neurodegenerative Diseases Group, Institute for Translational Research, Università della Svizzera Italiana, Ente Ospedaliero Cantonale, Bellinzona, Switzerland.

²Faculty of Biomedical Sciences, Università Della Svizzera Italiana, Lugano, Switzerland. ³Department of Pharmacological and Biomolecular Sciences, University of Milan, Milan, Italy. ⁴Department of Neuroscience, Istituto di Ricerche Farmacologiche Mario Negri IRCCS, Milan, Italy. ⁵Department of Life and Environmental Sciences, Marche Polytechnic University, Ancona, Italy. ⁶IRCCS Istituto delle Scienze Neurologiche di Bologna, 40126 Bologna, Italy. ⁷Department of Biomedical and NeuroMotor Sciences (DiBiNeM), University of Bologna, Bologna, Italy. ⁸Sleep Medicine Unit, Neurocenter of Southern Switzerland, Ente Ospedaliero Cantonale, Lugano, Switzerland. ⁹Department of Neurology, Cantonal Hospital St. Gallen, Switzerland. ¹⁰Department of Neurology, Inselspital, University Hospital Bern, Bern, Switzerland. ¹¹Neurology Department, Neurocenter of Southern Switzerland, Ente Ospedaliero Cantonale, Lugano, Switzerland. ¹²Department of Molecular Medicine, Laboratory Affiliated to Istituto Pasteur Italia - Fondazione Cenci Bolognetti, Sapienza University of Rome, Viale Regina Elena, 291, Rome, Italy.

¹³School of Biosciences, College of Health and Life Sciences, Aston University, Birmingham, B4 7ET, United Kingdom. ¹⁴Department of Health Policy, Istituto di Ricerche Farmacologiche Mario Negri IRCCS, Milan, Italy. ¹⁵These authors contributed equally: Elena Vacchi, Arianna Giani.

✉ e-mail: Giorgia.Melli@eoc.ch; Tiziana.Borsello@unimi.it

plays a critical role in disease progression and neurodegeneration. Moreover, although most PD cases are sporadic, genetic factors have been implicated in their development, potentially serving as early biological triggers^{5,6}.

PD diagnosis is primarily based on clinical evaluation, guided by either the UK Parkinson's Disease Society Brain or the refined International Movement Disorder Society (MDS) clinical diagnostic criteria^{7,8}. Although genetic testing can provide supportive evidence, the significant heterogeneity in PD's underlying causes makes early detection challenging. Initial clinical presentations are highly variable and often include non-motor symptoms such as anxiety, constipation, hyposmia, depression, and isolated rapid-eye-movement sleep behavior disorder (iRBD)⁷. Moreover, motor symptoms can take years to emerge (on average, about 10 years), thus delaying diagnosis². Recognizing the pre-motor phase is therefore crucial for developing disease-modifying treatments⁹, and the identification of reliable biomarkers for early detection and intervention remains a crucial challenge. Although no Biomarker has yet achieved full clinical validation, several promising approaches are under investigation. Notably, two strategies are currently being explored: (i) assessing α -Syn seeding capacity in cerebrospinal fluid (CSF) by seeding amplification assay and (ii) detecting phosphorylated α -Syn (P- α Syn) deposits in peripheral nerves via skin biopsy¹⁰. In fact, skin biopsy has emerged as a promising, non-invasive method to assess α -Syn pathology in peripheral tissues^{11,12}. Variations in CSF α -Syn seed and increases in its phosphorylated or aggregated forms in peripheral tissues might serve as indicators of disease progression. However, the lack of cohort studies and truly quantitative technology has hampered the development of prognostic markers¹². In addition, blood-based detection of Neurofilament Light Chain (NfL), a general biomarker of neuroaxonal injury, has been investigated for its potential to monitor disease progression in PD, even though it is not specific to this disorder¹³⁻¹⁵. In fact, NfL levels fall short in distinguishing PD from other neurodegenerative disorders¹⁴.

This unmet need for disease-specific peripheral biomarkers in PD provides a strong rationale to explore novel molecular pathways. Among others, JNK3 is a key member of the JNK kinase family, which also includes the JNK1 and JNK2 isoforms¹⁶, presenting a brain-specific expression pattern and functional variations that may offer valuable insights into the progression of PD. JNK3 has been shown to be strongly activated in several neurodegenerative diseases, including Alzheimer's disease (AD)^{17,18}, motor neuron disease¹⁹, epilepsy²⁰, and various other central nervous system (CNS) pathological conditions²¹⁻²³, as well as in PD^{24,25}. In PD, growing evidence highlights JNK3 as a key pathway driving neuronal death^{26,27}, and its selective inhibition has shown promising neuroprotective effects, both in vitro and in vivo^{28,29}, offering hope for therapeutic strategies. Notably, JNK3 plays a key role in regulating "synaptic injury", which is recognized as one of the earliest and most common neurodegenerative events^{17,18,30}. Beyond synaptic dysfunction, JNK3 also contributes to oxidative stress, inflammation, mitochondrial dysfunction, and apoptosis in dopaminergic neurons¹⁶. Despite its neuronal specificity, its activation in response to neuronal stress, and its involvement in regulating neuroinflammation and apoptosis, the potential of JNK3 as a PD biomarker remains largely unexplored. To date, only one study has reported elevated levels of JNK3 in the CSF of AD patients, where JNK3 levels significantly correlated with cognitive decline³¹. This finding provides the first clinical evidence that JNK3 can be released into extracellular fluids, supporting the hypothesis that JNK3 may also be detectable in other biofluids such as the blood.

Based on this, we investigated plasmatic JNK3 levels in PD patients at different stages of disease, including premotor phase (i.e., iRBD) and age-matched healthy controls (HC).

Results

Demographics and clinical characteristics

A total of 108 patients were enrolled and analyzed in this study; in detail, 25 iRBD, 26 De Novo PD, 29 Late PD patients, and 28 age-matched HC. The

demographic characteristics and clinical assessments of the study groups are summarized in Table 1.

No significant differences in age were found between groups, while a higher number of males was present in the iRBD group compared to the others, especially vs HC. As expected, De Novo and Late PD had higher motor impairment than iRBD, as measured by H&Y and MDS-UPDRS-III scale scores and LEDD. iRBD showed higher score at RBDSQ and major autonomic impairment vs Late PD measured by COMPASS-31, and hyposmia was significantly worse in De Novo PD than iRBD.

Plasmatic JNK3 is higher in patients with PD

Our results indicate that the neuronal isoform JNK3 is detectable in plasma and can be accurately measured using a commercial ELISA kit (see Materials and Methods for details). Plasma JNK3 concentrations were higher in iRBD and PD compared to HC (Fig. 1A). After adjustment for age and sex, multivariate logistic regression analysis demonstrated that higher plasma JNK3 levels were significantly associated with the diagnoses of iRBD, De Novo PD, and Late PD (Fig. 1B, upper panel). Consistent results were obtained with ordinal logistic regression, confirming that JNK3 expression rises progressively across these clinical stages (Fig. 1B, lower panel). In contrast, when LEDD was included as an additional covariate, the association between JNK3 levels and Late PD diagnosis was no longer significant in the comparison between Late PD and De Novo PD ($P = 0.203$). ROC curve analysis showed that plasmatic JNK3 concentration reliably distinguished HC from Late PD, achieving high specificity (100%) and moderate sensitivity (65.5%), while a lower sensitivity but same high specificity was obtained in separating De Novo vs HC (specificity 100%, sensitivity 50%) and iRBD vs HC (specificity 100%, sensitivity 48%) (Fig. 1C).

Plasmatic JNK3 is influenced by age and sex

In HC, plasmatic JNK3 levels showed an inverse correlation with age ($p = 0.013$, $B = -0.078$, Fig. 2A). In addition, its expression resulted significantly lower in females than males, and this trend was also detectable in the other groups (iRBD $p = 0.496$, De Novo $p = 0.879$, and Late PD $p = 0.784$, (Fig. 2B-E). When comparing males and females within each group, the increase in plasma JNK3 expression observed in patients relative to HC remained evident but was less pronounced among males (global ANOVA: 0.0950; no linear tests between groups since global test not significant) (Fig. 2F) than in females (global ANOVA: 0.0004) (Fig. 2G). In the combined analysis of De Novo and Late PD patients, plasma JNK3 levels did not correlate significantly with age (Fig. 2H). In contrast, a significant positive correlation with age was observed when the analysis was restricted to the Late PD group ($p = 0.048$, $B = 0.105$; Fig. 2I). Moreover, JNK3 levels showed a significant negative correlation with the motor scale MDS-UPDRS-III, observed when grouping De Novo and Late PD ($p = 0.027$, $B = -0.074$) (Fig. 2J).

Association between JNK3 and α -synuclein pathology

The same patients underwent both skin biopsy and blood sampling, allowing for a direct correlation between peripheral α -Syn pathology and plasma JNK3 levels. Immunofluorescence analysis of P- α Syn in skin biopsies showed positivity in 13.3% of HC, 62.5% iRBD, 77.8% De Novo PD, and 68.2% of Late PD. When participants were stratified by skin-biopsy positivity for P- α Syn (Fig. 3A-C), those who resulted positive (57.1%) displayed significantly higher plasma JNK3 levels (Fig. 3D). This association was confirmed considering iRBD and PD at different stages (70.8% positive, Fig. 3E) as well as only Late PD (68.2% positive, Fig. 3F).

Our bioinformatic analysis specifically investigated the interaction pathways of JNK3 and α -Syn (SNCA) and revealed that the scaffold protein mitogen-activated protein kinase 8 interacting protein 1 (MAPK8IP1, also *JNK-interacting protein 1 (JIP1)*) occupies a central hub position, connecting the JNK kinase family with α -Syn (i.e., SNCA) (Fig. 4A). Network analysis of overlapping neurodegenerative pathways in PD and AD identified JIP1 as a central mediator linking the two diseases (Fig. 4B). These findings suggest that JNK3 may interact with α -Syn through JIP1, potentially contributing to

Table 1 | Demographic and clinical characteristics of iRBD and different PD stages

	HC (n = 28)	iRBD (n = 25)	De Novo (n = 26)	Late PD (n = 29)	HC vs iRBD	HC vs De Novo	HC vs Late PD	iRBD vs De Novo	iRBD vs Late PD	De Novo vs Late PD
Age (y)	64.8 ± 9.9	65.7 ± 7.7	64.2 ± 11.4	66.0 ± 11.5	0.965	0.946	0.949	0.880	0.896	0.859
Biological Sex (%)M	50.0	80.0	69.0	69.0	0.029	0.147	0.182	0.288	0.272	0.607
BMI	23.9 [22.3-26.4]	26.3 [23.4-28.0]	24.9 [22.7-29.7]	24.7 [21.6-27.3]	0.065	0.278	0.810	0.694	0.128	0.415
Age of onset (y)	—	63.5 ± 8.1	62.7 ± 11.5	59.5 ± 13.1	—	—	—	0.778	0.270	0.314
Disease duration(y)	—	2.6 ± 1.6	1.8 ± 1.0	6.4 ± 3.1	—	—	—	0.570	0.000	0.000
H&Y	—	1.0 [1.0-1.0]	1.0 [1.0-2.0]	2.0 [2.0-3.0]	—	—	—	0.009	0.000	0.003
UPDRS-I	—	6.5 [2.5-17.8]	11.0 [3.0-14.5]	5.5 [4.0-7.8]	—	—	—	0.550	0.790	0.245
UPDRS-II	—	1.0 [0.0-6.0]	5.0 [3.0-10.5]	6.5 [3.3-8.0]	—	—	—	0.042	0.019	0.937
UPDRS-III	—	6.0 [4.0-8.0]	15.0 [10.0-24.0]	11.5 [7.8-17.5]	—	—	—	0.000	0.004	0.157
UPDRS-TOT	—	13.5 [5.8-37.3]	29.0 [21.5-50.0]	24.5 [17.5-36.5]	—	—	—	0.075	0.196	0.256
COMPASS-31_OH	—	0.0 [0.0-12.0]	0.0 [0.0-16.0]	0.0 [0.0-6.0]	—	—	—	0.566	0.440	0.167
COMPASS-31_VM	—	0.0 [0.0-0.0]	0.0 [0.0-0.0]	0.0 [0.0-0.0]	—	—	—	0.211	0.398	0.616
COMPASS-31_SM	—	1.5 [0.0-4.2]	2.1 [0.0-4.2]	0.5 [0.0-4.2]	—	—	—	0.947	0.607	0.555
COMPASS-31_GI	—	4.5 [0.0-6.3]	4.9 [1.6-7.7]	1.8 [0.0-5.3]	—	—	—	0.518	0.129	0.020
COMPASS-31_BL	—	0.0 [0.0-2.1]	0.0 [0.0-1.1]	0.0 [0.0-1.1]	—	—	—	0.333	0.156	0.617
COMPASS-31_PM	—	0.8 [0.0-1.3]	0.0 [0.0-1.5]	0.0 [0.0-0.0]	—	—	—	0.799	0.014	0.030
COMPASS-31_TOT	—	14.2 [6.6-22.7]	8.8 [4.8-27.3]	7.1 [0.5-13.5]	—	—	—	0.788	0.047	0.098
Beck_Depr	—	8.0 [2.8-11.0]	8.0 [3.5-17.0]	5.0 [3.0-9.5]	—	—	—	0.578	0.412	0.095
MMSE	—	29.0 [28.0-30.0]	30.0 [28.5-30.0]	30.0 [29.0-30.0]	—	—	—	0.229	0.037	0.464
MoCA	—	26.0 [21.0-28.0]	26.0 [22.0-28.5]	29.0 [25.0-29.0]	—	—	—	0.888	0.012	0.028
Smell test	—	8.0 [6.0-10.0]	6.0 [3.5-8.0]	7.0 [4.0-9.5]	—	—	—	0.042	0.305	0.346
RBDSQ	—	10.0 [8.8-10.5]	3.0 [2.0-6.5]	4.0 [1.5-5.5]	—	—	—	0.000	0.000	0.820
LEDD	—	0.0 [0.0-0.0]	7.0 [0.0-187.1]	552.0 [302.5-725.0]	—	—	—	0.000	0.000	0.000

Variables are reported as mean ± SD, median [interquartile range], and absolute number (percentage), as appropriate. A p-value < 0.05 was shown in bold.

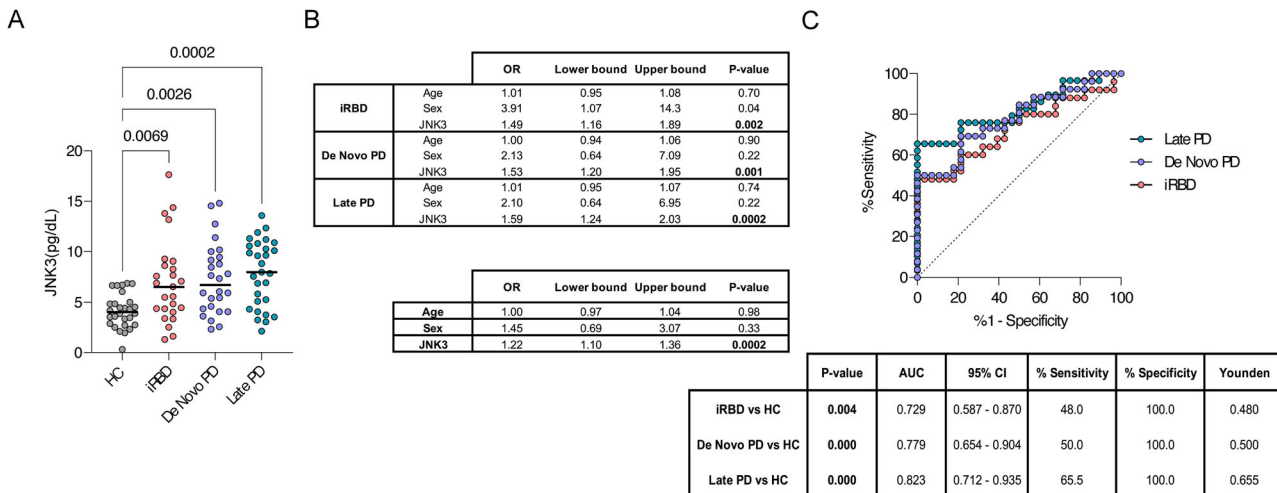


Fig. 1 | Evaluation of plasmatic JNK3 as a promising diagnostic biomarker. A Plot of plasmatic JNK3 concentration measured by ELISA assay in HC and pathological groups. Each dot represents a patient and bars the median of the group. Significant pairwise Bonferroni corrected *P*-values, after one-way ANOVA analysis, are shown. Multivariate multinomial (B, upper panel) and ordinal logistic regression (B, lower

panel) analyses to assess the OR and 95% CI for JNK3, age, and sex among pathological groups. An OR > 1 indicates an increased likelihood of pathological diagnosis. C ROC curves analysis of JNK3 concentration. The referral line is reported in black. For each comparison, the table provides the asymptotic significance, AUC with 95% CI, % sensitivity, specificity, and Youden value.

shared pathogenic mechanisms and supporting its role as a candidate biomarker for PD.

Plasmatic NfL evaluation across PD stages

Neither parametric (ANOVA) nor non-parametric (Kruskall-Wallis) analysis revealed a difference of NfL concentration, measured by SIMOA, among the four groups, even though a slight monotone ascending trend was visible from HC to PD (Fig. 5A). These results were confirmed in multivariate logistic analyses: multinomial analysis did not reach significance, while ordinal analysis found a slight significance ($p = 0.020$) at univariate level, which remained significant ($P = 0.011$) after correcting for age and gender (Fig. 5B). Furthermore, NfL values strongly correlated with age ($p < 0.001$, $B = 0.032$) across all groups (Fig. 5C). NfL also correlated with motor impairment when grouping De Novo and Late PD patients (as per the H&Y scale) (Fig. 5D), while correlated with depression in Late PD group (as per the BDI-II scale) (Fig. 5E).

Discussion

PD remains a diagnostic and prognostic challenge, largely due to the lack of accessible, reliable biomarkers and the great heterogeneity of clinical phenotypes. The lack of a clear link between PD clinical manifestations and currently available biomarker profiles hampers early diagnosis and precise disease monitoring, underscoring the need for novel biomarkers that more accurately reflect PD pathophysiology. Our study highlights plasmatic quantification of neuronal kinase JNK3 as a promising peripheral biomarker for PD.

Our findings show that plasma JNK3 levels can be reliably measured and are increased early in the PD continuum, including in individuals with iRBD, a prodromal stage marked by non-motor symptoms and subtle neurodegeneration. These findings are derived from plasma measurements of JNK3 and therefore do not allow direct conclusions regarding its mechanistic role in early neurodegenerative processes. Nonetheless, the significant elevation of JNK3 in iRBD, exceeding that of NfL, suggests that it may serve as a marker of early neuronal stress and/or synaptic dysfunction. This interpretation is consistent with the established role of JNK3 in neuronal death pathways and is further supported by bioinformatic analyses indicating its involvement within neurodegeneration-related interactomes, reinforcing JNK3 as a promising and potentially druggable target for neuroprotective interventions^{17,21,32}. The elevation of NfL is associated with neuroaxonal degeneration and fast disease progression and is particularly

relevant in motor neuron disorders³³. In PD, however, studies have reported mixed results, some indicating higher plasma NfL levels in patients compared with HC, while others found no significant difference³⁴. Even when present, NfL increase in PD is generally modest, particularly in the early stages of the disease³⁵, consistent with the findings of the present work.

In addition, the progressive increase in JNK3 levels from iRBD through De Novo to Late PD further supports its potential as a dynamic biomarker capable of tracking neurodegenerative changes across disease stages. Notably, plasma JNK3 levels distinguished all stages of PD and iRBD from HC with high specificity (100%) and moderate sensitivity (48–65%), being higher for Late PD (65%). Although the Youden method yields perfect specificity, this comes at the expense of a moderate sensitivity. Adjusting the balance between sensitivity and specificity may therefore be considered, depending on the clinical context and the associated cost-benefit considerations.

Plasma JNK3 is a promising, non-invasive biomarker that overcomes the limitations of invasive CSF-based markers. Its accessibility via routine blood sampling allows for longitudinal monitoring of disease progression and could facilitate earlier patient stratification for clinical trials. Although quantification would be enhanced by a more sensitive, SIMOA-based assay (not yet commercially available), current measurement relies on well-established laboratory techniques. This simplicity ensures that plasma JNK3 can be readily integrated into existing diagnostic workflows, accelerating its clinical translation.

In HC, we observed that JNK3 levels decreased with age and were lower in females, a trend consistent with physiological brain aging³⁶. Notably, this is in direct contrast to plasma NfL, which increased with age, confirming previous studies^{13–15}. This opposing trajectory suggests that JNK3 and NfL are controlled by distinct biological mechanisms during the aging process. In patients with PD, however, this age-related decline in JNK3 was reversed, indicating that the effects of neurodegeneration override the normal aging process, and positioning JNK3 as a potential marker of disease-specific pathology rather than a general biomarker of aging. Further studies are required to validate this hypothesis.

Counter-intuitively, despite being elevated in the PD cohort, higher JNK3 levels were associated with lower motor impairment. This may indicate that JNK3 does not track motor decline directly, but rather reflects other aspects of the disease, such as non-motor pathology. Indeed, its early elevation in iRBD further supports the notion that JNK3 serves as a sensitive marker of early neuronal dysfunction, potentially reflecting synaptic

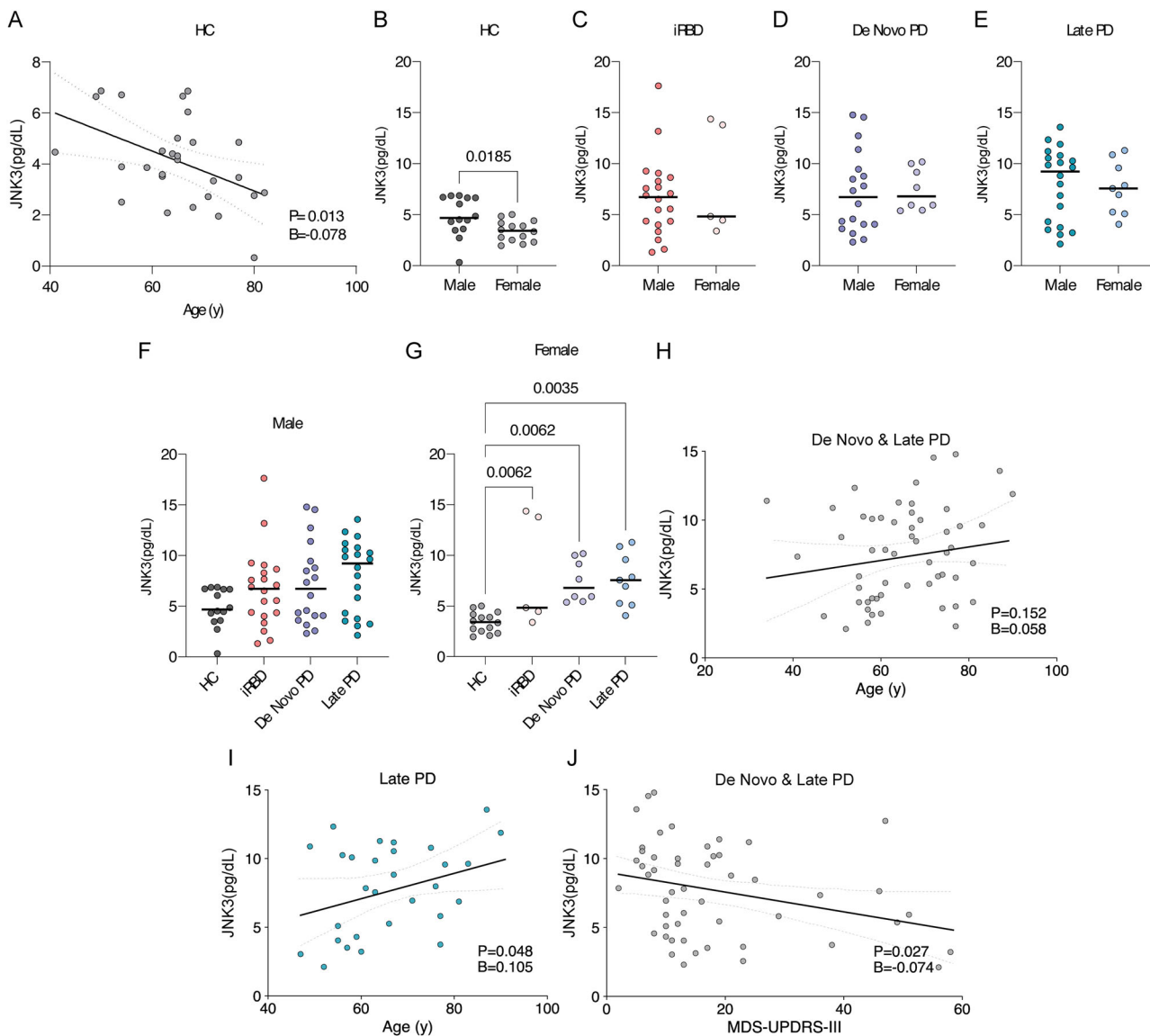


Fig. 2 | Clinical correlations and sex influence on JNK3 levels. **A** Correlation between JNK3 and age in HC. **B–G** Scatter plot of plasmatic JNK3 concentration in males and females in the distinct groups. Each dot represents a patient and bars the median of the group. Unpaired T-Test and one-way ANOVA analyses are shown.

P-values < 0.05 were considered significant. **H, I** Correlation between JNK3 and age. **J** Correlation between JNK3 and MDS-UPDRS-III in De Novo and Late PD. The regression lines are reported together with their 95% CI (dashed line).

impairment and involvement of extra-motor regions, components that are overlooked in motor-centric PD assessments. Furthermore, the limitations of motor assessments in levodopa-treated individuals may obscure the true relationship between the biomarker and underlying neurodegeneration, potentially explaining this unexpected finding. Further studies with larger cohorts and more comprehensive clinical characterization will be required to confirm this association and clarify its biological significance.

A key finding of this study is the strong correlation between plasma JNK3 and peripheral P- α Syn derived from skin biopsies within the same individuals. This paired analysis establishes a direct link between a CNS-related blood biomarker and peripheral synucleinopathy. The convergence of these two markers supports a potential dual-biomarker strategy for improved early diagnosis and disease monitoring, offering a powerful, minimally invasive alternative to lumbar punctures or neuroimaging. The established reliability of skin P- α Syn as a diagnostic marker further strengthens the clinical potential of this combined approach³.

This preliminary study is limited by its small sample size, and our findings require validation in larger, independent cohorts. Future studies should aim to correlate plasma JNK3 with advanced neuroimaging^{37,38} and

other fluid biomarkers (e.g., α -Syn species, synaptic proteins³⁹) to better contextualize its pathological role. Longitudinal studies will be crucial to determine if JNK3 can track disease progression, predict clinical outcomes, or monitor therapeutic responses, particularly in diverse cohorts such as atypical parkinsonisms, α -Syn-negative PD subtypes, and patients undergoing disease-modifying therapies. Finally, mechanistic studies exploring the link between plasma JNK3, skin P- α Syn, as well as JNK3 presence in other tissues like CSF are needed to fully understand its biological significance. Addressing these points will clarify how to best integrate JNK3 into multiparametric panels to improve diagnosis, stratification, and personalized medicine for PD.

Methods

Patients' enrollment

Patients were consecutively recruited from the movement disorders and sleep medicine clinic at NSI Lugano, the sleep medicine clinic at the University-Hospital of Bologna, and the movement disorders clinic at St. Gallen Hospital, as part of the multicentric NSIPD001 study. HC were recruited among hospital staff and patients' partners. Inclusion criteria for

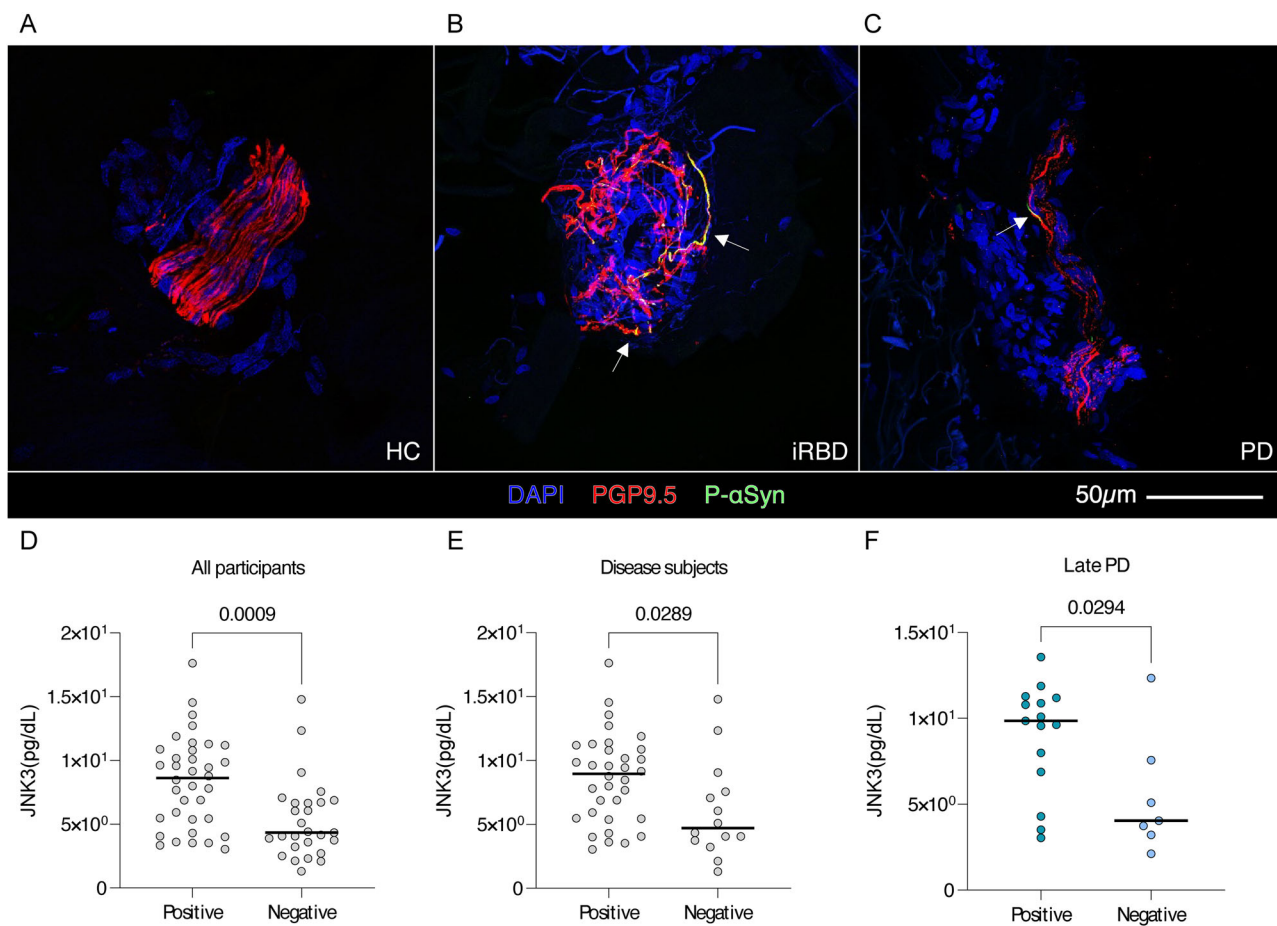


Fig. 3 | Differences of JNK3 in patients positive for cutaneous phosphorylated α -Syn. Confocal microscopy images of a muscle arrector pili in HC (A), sweat gland in iRBD (B), and dermal plexus in PD (C). The co-localization signal of P- α Syn (green) and nerve fibers (red) is defined by the yellow signal (white arrows). Scale bar: 50 μ m

(D–F) Plot of plasmatic JNK3 concentration in subjects positive or negative for P- α Syn. Each dot represents a patient and bars the median of the group. Unpaired T-test analysis is shown.

PD were a definite clinical diagnosis according to the UK Brain Bank diagnostic criteria⁴⁰, and no family history. De Novo PD were patients with less than 2 years from the diagnosis, while Late PD were patients with >2 and <15 years from the diagnosis. Inclusion criteria for iRBD were established according to the standard diagnostic criteria and included a video-polysomnography documentation of REM sleep without atonia⁴¹.

Clinical assessment

Patients underwent a standard clinical evaluation: Hoehn and Yahr scale (H&Y)⁴² and the Movement Disorder Society-Unified Parkinson's Disease Rating Scale (MDS-UPDRS)⁴³ were used for disease gravity assessment; Mini-Mental State Evaluation (MMSE)⁴⁴ and Montreal Cognitive Assessment (MoCA)⁴⁵ scales for cognitive impairment; Beck Depression Inventory-II (BDI-II)⁴⁶ scale for mood disorder; Composite Autonomic Symptom Score 31 (COMPASS-31, OH: orthostatic hypotension, VM: vasomotor, SM: sudomotor, GI: gastrointestinal, BL: bladder, PM: pupillomotor)⁴⁷ for autonomic dysfunction; rapid eye movement (REM) sleep behavior disorder screening questionnaire (RBDSQ) for REM sleep disorders⁴⁸. Levodopa equivalent daily dose (LEDD)⁴⁹ was calculated for PD patients. The BMI was also reported.

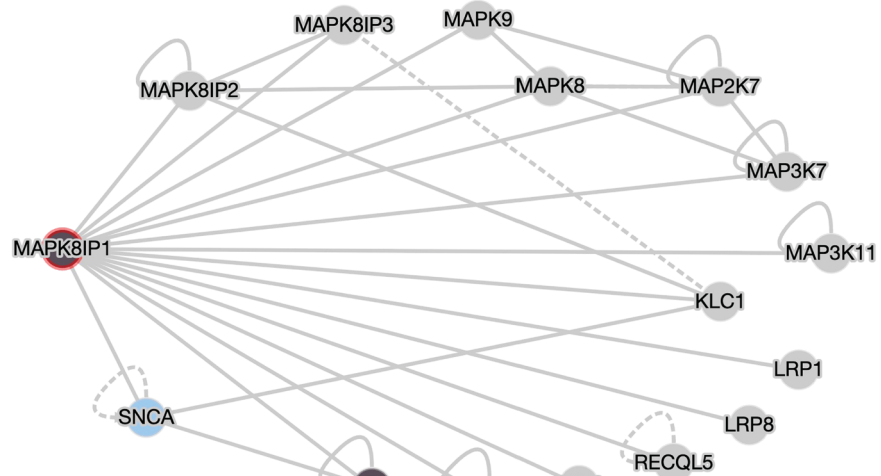
Blood collection and plasma preparation

All subjects included in the study underwent blood collection. 10 ml of blood were collected into anticoagulant-EDTA tubes and centrifuged for 15 minutes at 1600 g at 10 °C, to eliminate cellular components. The obtained plasma was aliquoted and stored at –80 °C.

JNK3 ELISA

JNK3 level detection in plasma was performed using the Human Stress-activated Protein Kinase JNK3, MAPK10 commercial ELISA kit (Bioassay Technology Laboratory, EA701Hu) distributed by Li Starfish (Catalog number: BTB-E6701HU; https://www.bt-laboratory.com/index.php/Shop/Index/productShijiheDetail/p_id/29125.html; Datasheet: <https://www.bt-laboratory.com/Upload/manual/kit/E6701Hu.pdf>). Plasma samples were collected as described in the Blood Collection and Plasma Preparation section, aliquoted, and stored at –80 °C, avoiding repeated freeze–thaw cycles. Only one freeze–thaw cycle was allowed before measurement. Plasma samples were not diluted when using this ELISA kit. When sediments were observed after storage, samples were centrifuged again before analysis and hemolyzed samples were excluded. All analyses were performed in triplicate and using two different kit batches to minimize variability. Before use, all reagents and samples were equilibrated to room temperature for 30 minutes. Disposable pipette tips and plate sealers were used to prevent cross-contamination. According to the manufacturer's specifications, the assay has a sensitivity of 13.19 ng/L, with a standard curve range of 20–6000 ng/L. The intra-assay coefficient of variation (CV) is reported to be < 8% and the inter-assay CV < 10%. The assay is validated for use with plasma samples. Although no independent spike-in recovery tests were performed in this study, and the manufacturer does not provide recovery data in plasma, all measured values in our samples were within the validated detection range. This product is for research use only, not for use in a diagnostic procedure as described in the manufacturer's protocol.

A



B

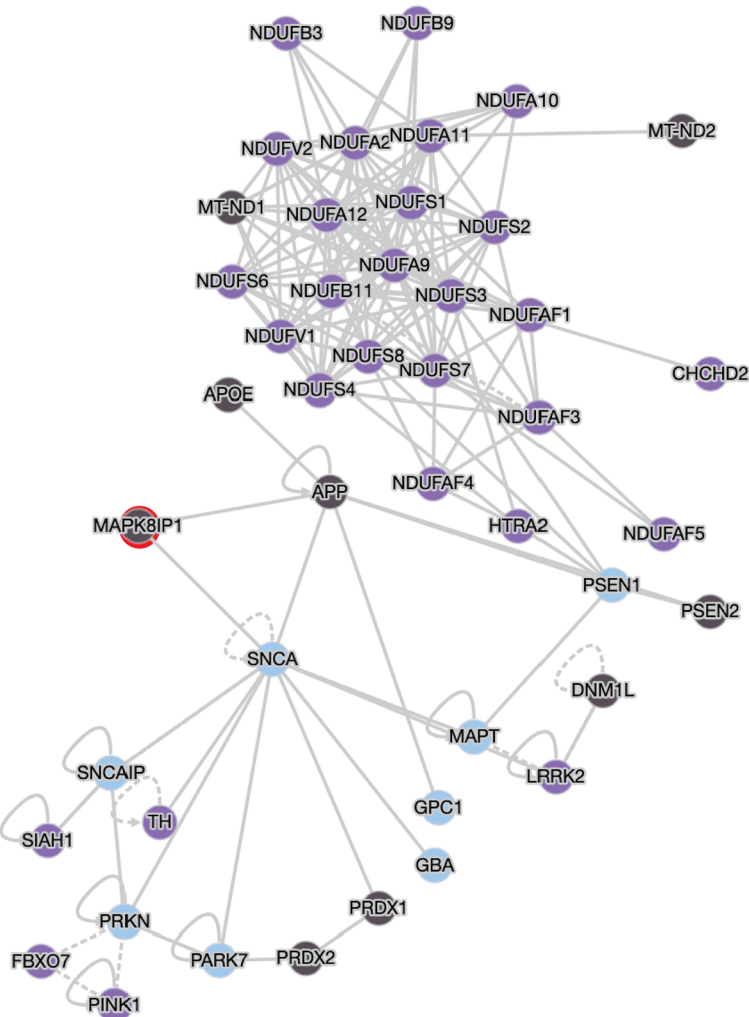


Fig. 4 | Network integration of the neurodegeneration-related interactome from NDAtlas. **A** Interaction network centered on MAPK8IP1 (JIP1), illustrating its connectivity with JNK kinases (MAPK9 and MAPK8), and α -Syn (SNCA). **B** Overlapping interaction networks of PD and AD highlighting the central connectivity role of MAPK8IP1 (JIP1). Interaction metrics: MAPK8IP1-SNCA Score:

0.6655, Confidence: 0.3010. Each node indicates a protein or gene associated with a neurodegenerative disease, color-coded as follows: gray for N/A, black for AD, blue for multiple pathologies, and purple for PD. Edges (lines) between nodes represent known or predicted interactions, such as physical binding or functional links.

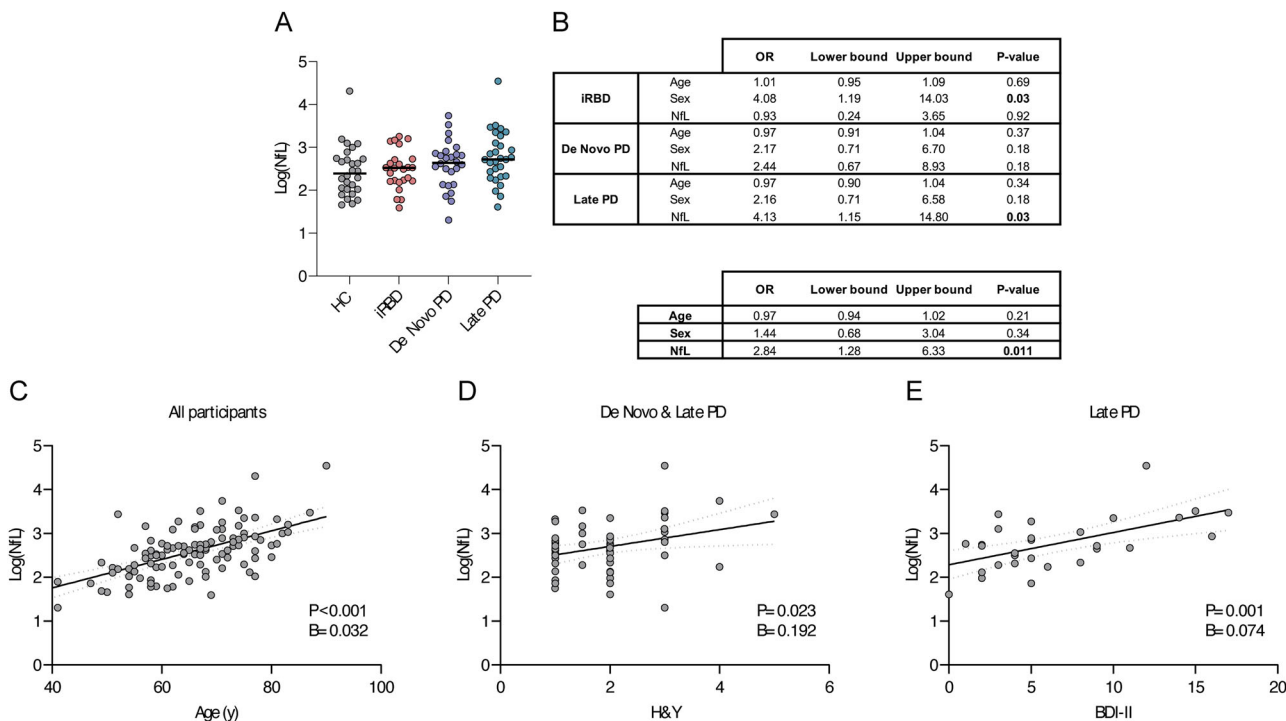


Fig. 5 | Evaluation of plasmatic NfL in the study cohort. **A** Plot of plasmatic log(NfL) concentration measured by SIMOA technology in HC and pathological groups. Each dot represents a patient and bars the median of the group. **(B, upper panel)** Multivariate multinomial and **(B, lower panel)** ordinal logistic regression analyses to assess the OR and 95% CI for NfL, age, and sex among pathological

groups. An OR > 1 indicates an increased likelihood of pathological diagnosis. **C** Correlation between log(NfL) and age in all participants. **D** Correlation between log(NfL) and H&Y in De Novo and Late PD groups. **E** Correlation between log(NfL) and BDI-II in Late PD group. For all correlations, the regression line is reported together with its 95% CI (dashed line).

Plasma NfL quantification

The plasma NfL was quantified using a Simoa NF-Light Advantage PLUS (SR-X) Kit (#104364) on a Quanterix SR-X platform (Quanterix, Boston, MA, USA). All reagents used for NfL analysis were from a single lot, and measurements were performed according to the manufacturer's protocol.

Skin biopsy collection and immunofluorescence

Based on the availability of the biobank, skin biopsy has been performed in 43.6% of HC (15 out of 28), 32.0% of iRBD (8 out of 25), 69.2% of De Novo PD (18 out of 26), and 75.9% of Late PD (22 out of 29). A 3 mm-diameter punch skin biopsy was performed in the neck at C8 dermatomal level (cervical) and in the distal leg 10 cm above the lateral malleolus (ankle). Following our published and standardized protocol^{11,12}, skin samples were fixed overnight at 4 °C in Paraformaldehyde-lysine-periodate (PLP) 2% fixative. The day after, 50-μm-thin skin sections were cut with a cryotome for free-floating immunofluorescence analysis. Three non-consecutive sections per localization per patient were incubated overnight with antibodies against the panaxonal marker protein gene product 9.5 (PGP9.5, rabbit, polyclonal, EMD Millipore Corporation, AB5925, dilution 1:1000) and P-αSyn at serine 129 (mouse, monoclonal, FUJIFILM Wako Pure Chemical Corporation, 015-25191, dilution 1:1000). The day after, sections were incubated with secondary antibodies AlexaFluor488 and AlexaFluor594 (ThermoFisher Scientific, Waltham, USA, 1:1000), and counterstained with DAPI. All samples were anonymized and coded before the arrival in the laboratory; thus, staining, imaging acquisition, and analysis were performed by operators blinded to the clinical diagnosis^{11,12}.

Immunofluorescence evaluation

Skin sections were evaluated under an inverted fluorescence microscope (Nikon Eclipse Ti-E, Tokyo, Japan). For each section, intraepidermal nerve fibers, dermal nerve bundles, and at least 15 autonomic structures (sweat glands, muscle arrector pili, and vessels)

per anatomical area per patient were screened. Structures showing P-αSyn signal within PGP9.5 positive nerve fibers were further analyzed using a confocal microscope (Leica Stellaris 5, LasX software). Serial pictures, every 2 μm on the Z-axis, were taken using a 40X magnification. Every single stack of all the obtained pictures was analyzed with ImageJ software by an operator blinded to the clinical diagnosis. To ensure consistency, all evaluations were performed using standardized image acquisition and analysis parameters. For each image, the presence/absence of P-αSyn signal was reported. Structures were defined as “positive” if showing P-αSyn within PGP9.5-positive fibers. Anatomical sites were defined as “positive” when at least one positive structure was present. A subject was considered P-αSyn positive if at least one PGP9.5-positive structure containing P-αSyn immunoreactivity was detected in any of the sampled sites.

Bioinformatic analysis

Protein-protein interaction investigation was conducted using the Neurodegenerative Disease Atlas (NDAtlas) database (accessed March 24, 2025; <https://bis.zju.edu.cn/ndatlas/>). NDAtlas integrates protein-protein interaction data, structural docking scores, isoform information, and disease-specific subnetworks to provide a comprehensive, high-resolution interactome map⁵⁰.

Statistical analysis

Statistical analysis was performed using IBM SPSS Statistics 26.0 and Stata/IC v 15.1. Variable distribution was assessed by the Kolmogorov-Smirnov test. One-way ANOVA test with post-hoc Bonferroni's test for multiple comparisons was used for normally distributed variables, with descriptive statistics expressed as mean ± standard deviation (SD); Kruskal-Wallis test for non-normally distributed variables, with descriptive statistics expressed as medians and interquartile range; χ^2 or Fisher's exact tests for categorical variables, reporting frequencies and percentages (%). We looked at the graphical distribution to obtain a view of the approximate normality of the

variables of interest. Since the graphs showed the presence of skewness or a few extreme (high) values, we tried a logarithmic transformation to obtain a normal distribution. We also used a formal test (Royston, P. 1991. sg3.5: Comment on sg3.4 and an improved D'Agostino test. Stata Technical Bulletin 3: 23-24. Reprinted in Stata Technical Bulletin Reprints, vol. 1, pp. 110-112. College Station, TX: Stata Press): logarithmic transformation of NfL and original scale of JNK3 had best results and were used for parametric analyses, even though they were slightly non-normal, since parametric analyses are rather robust for slight deviations from normality and necessary to conduct more flexible analyses. Multivariate multinomial logistic regression analysis, adjusted for age and sex, was performed to evaluate differences between the different diagnostic stages and HC. Since the different classes were ordered, we also used an ordered multivariate logistic regression to obtain a single parameter to study the association between JNK3 or NfL and PD/HC classes; the assumption of proportionality across the categories was tested without finding any departure. A model further correcting for BMI was implemented but disregarded since some subjects had no BMI value and, at the same time, BMI did not show any correlation with PD stages, neither at univariate nor multivariate levels. ROC curve analysis was used to evaluate the area under the curve (AUC) and compare diagnostic performances. In addition to AUC, *p*-value, 95% confidence interval (CI), sensitivity, specificity, and Youden value were reported for each ROC analysis. Correlations were evaluated by Pearson's *r* coefficient and tested by univariate and multivariate linear regression analysis. A *p*-value lower than 0.05 was considered significant. The sample size of the study was dictated by the number of available plasmas. For clinical variables, missing data were not replaced, while JNK3 data were available for all subjects. Since values for plasmatic NfL were highly asymmetric, showing important outliers, we analyzed them after a logarithmic transformation, obtaining a much more symmetric distribution. Moreover, in relation to age, NfL showed heteroskedasticity while log(NfL) did not. JNK3 values were expressed as pg dL to obtain clinically interpretable parameter.

Ethics approval and consent to participate

This study was performed in line with the principles of the Declaration of Helsinki. Subjects were included according to the study protocol, approved by the Cantonal Ethics Committee (CETi 2895). All enrolled subjects gave written informed consent to the study.

Data availability

The data obtained in this research are available from the corresponding author upon reasonable request.

Received: 24 September 2025; Accepted: 18 November 2025;

Published online: 10 December 2025

References

- Zhu, J. et al. Temporal trends in the prevalence of Parkinson's disease from 1980 to 2023: a systematic review and meta-analysis. *Lancet Healthy Longev.* **5**, e464–e479 (2024).
- Bloem, B. R., Okun, M. S. & Klein, C. Parkinson's disease. *Lancet* **397**, 2284–2303 (2021).
- Höglinger, G. U. et al. A biological classification of Parkinson's disease: the SynNeurGe research diagnostic criteria. *Lancet Neurol.* **23**, 191–204 (2024).
- Simuni, T. et al. A biological definition of neuronal α -synuclein disease: towards an integrated staging system for research. *Lancet Neurol.* **23**, 178–190 (2024).
- Kalia, L. V. & Lang, A. E. Parkinson's disease. *Lancet* **386**, 896–912 (2015).
- Singleton, A. B., Farrer, M. J. & Bonifati, V. The genetics of Parkinson's disease: progress and therapeutic implications. *Mov. Disord.* **28**, 14–23 (2013).
- Chopra, A., Lang, A. E., Höglinger, G. & Outeiro, T. F. Towards a biological diagnosis of PD. *Parkinsonism Relat. Disord.* **122**, 106078 (2024).
- Postuma, R. B. et al. MDS clinical diagnostic criteria for Parkinson's disease. *Mov. Disord.* **30**, 1591–1601 (2015).
- Stocchi, F., Bravi, D., Emmi, A. & Antonini, A. Parkinson disease therapy: current strategies and future research priorities. *Nat. Rev. Neurol.* **20**, 695–707 (2024).
- Gibbons, C. H. et al. Skin biopsy detection of phosphorylated α -synuclein in patients with synucleinopathies. *JAMA* **331**, 1298 (2024).
- Melli, G. et al. Cervical skin denervation associates with alpha-synuclein aggregates in Parkinson disease. *Ann. Clin. Transl. Neurol.* **5**, 1394–1407 (2018).
- Vacchi, E. et al. Alpha-synuclein oligomers and small nerve fiber pathology in skin are potential biomarkers of Parkinson's disease. *NPJ Parkinsons Dis.* **7**, 119 (2021).
- Pedersen, C. C. et al. Serum neurofilament light at diagnosis: a prognostic indicator for accelerated disease progression in Parkinson's Disease. *NPJ Parkinsons Dis.* **10**, 162 (2024).
- Mollenhauer, B. et al. Validation of serum neurofilament light chain as a biomarker of Parkinson's disease progression. *Mov. Disord.* **35**, 1999–2008 (2020).
- Ygland Rödström, E., Mattsson-Carlgren, N., Janelidze, S., Hansson, O. & Puschmann, A. Serum neurofilament light chain as a marker of progression in parkinson's disease: long-term observation and implications of clinical subtypes. *J. Parkinsons Dis.* **12**, 571–584 (2022).
- Zeke, A., Misheva, M., Reményi, A. & Bogoyevitch, M. A. JNK signaling: regulation and functions based on complex protein-protein partnerships. *Microbiol. Mol. Biol. Rev.* **80**, 793–835 (2016).
- Musi, C. A., Agrò, G., Santarella, F., Iervasi, E. & Borsello, T. JNK3 as therapeutic target and biomarker in neurodegenerative and neurodevelopmental brain diseases. *Cells* **9**, 2190 (2020).
- Yoon, S. O. et al. JNK3 perpetuates metabolic stress induced by α β peptides. *Neuron* **75**, 824–837 (2012).
- Genabai, N. K. et al. Genetic inhibition of JNK3 ameliorates spinal muscular atrophy. *Hum Mol Genet.* **24**, 6986–7004 (2015).
- Yang, D. D. et al. Absence of excitotoxicity-induced apoptosis in the hippocampus of mice lacking the Jnk3 gene. *Nature* **389**, 865–870 (1997).
- Resnick, L. & Fennell, M. Targeting JNK3 for the treatment of neurodegenerative disorders. *Drug Discov. Today* **9**, 932–939 (2004).
- Chintala, S. K., Putris, N. & Geno, M. Activation of TLR3 promotes the degeneration of retinal ganglion cells by upregulating the protein levels of JNK3. *Invest Ophthalmol. Vis. Sci.* **56**, 505–514 (2015).
- de Lemos, L. et al. Neuroprotective effects of the absence of JNK1 or JNK3 isoforms on kainic acid-induced temporal lobe epilepsy-like symptoms. *Mol. Neurobiol.* <https://doi.org/10.1007/s12035-017-0669-1> (2017).
- Coffey, E. T. Nuclear and cytosolic JNK signalling in neurons. *Nat. Rev. Neurosci.* **15**, 285–299 (2014).
- Hunot, S. et al. JNK-mediated induction of cyclooxygenase 2 is required for neurodegeneration in a mouse model of Parkinson's disease. *Proc. Natl. Acad. Sci.* **101**, 665–670 (2004).
- Chen, Y., Zheng, X., Wang, Y. & Song, J. Effect of PI3K/Akt/mTOR signalling pathway on JNK3 in Parkinsonian rats. *Exp. Ther. Med.* <https://doi.org/10.3892/etm.2018.7120> (2018).
- Pan, J. et al. Small Peptide Inhibitor of JNK3 protects dopaminergic neurons from MPTP induced injury via inhibiting the ASK1~JNK3 signalling pathway. *PLoS ONE* **10**, e0119204 (2015).
- Shuai, W. et al. Selective covalent inhibiting JNK3 by small molecules for Parkinson's diseases. *Angew. Chem. Int. Edn.* **63**, <https://doi.org/10.1002/anie.202411037> (2024).
- Shuai, W. et al. Discovery of novel indazole chemotypes as isoform-selective JNK3 inhibitors for the treatment of Parkinson's disease. *J. Med. Chem.* **66**, 1273–1300 (2023).
- Camins, A. Role of JNK isoforms in the kainic acid experimental model of epilepsy and neurodegeneration. *Front. Biosci.* **22**, 4517, <https://doi.org/10.2741/4517> (2017).

31. Gourmaud, S. et al. Increased levels of cerebrospinal fluid JNK3 associated with amyloid pathology: links to cognitive decline. *J. Psychiatry Neurosci.* **40**, 151–161 (2015).
32. Wu, Y. et al. JNK3 inhibitors as promising pharmaceuticals with neuroprotective properties. *Cell Adh. Migr.* **18**, 1–11 (2024).
33. Zucchi, E. et al. Neurofilaments in motor neuron disorders: towards promising diagnostic and prognostic biomarkers. *Mol. Neurodegener.* **15**, 58 (2020).
34. Buhmann, C., Magnus, T. & Choe, C.-U. Blood neurofilament light chain in Parkinson's disease. *J. Neural Transm. (Vienna)* **130**, 755–762 (2023).
35. Lin, C.-H. et al. Blood NfL: A biomarker for disease severity and progression in Parkinson disease. *Neurology* **93**, e1104–e1111 (2019).
36. Li, Y. et al. c-Jun N-terminal kinase signaling in aging. *Front Aging Neurosci.* **16**, <https://doi.org/10.3389/fnagi.2024.1453710> (2024).
37. Orso, B. et al. Progression trajectories from prodromal to overt synucleinopathies: a longitudinal, multicentric brain [18F]FDG-PET study. *NPJ Parkinsons Dis.* **10**, 200 (2024).
38. Holmes, S. E. et al. Synaptic loss and its association with symptom severity in Parkinson's disease. *NPJ Parkinsons Dis.* **10**, 42 (2024).
39. Nilsson, J. et al. Cerebrospinal fluid biomarkers of synaptic dysfunction are altered in Parkinson's disease and related disorders. *Movement Disord.* **38**, 267–277 (2023).
40. Hughes, A. J., Daniel, S. E., Kilford, L. & Lees, A. J. Accuracy of clinical diagnosis of idiopathic Parkinson's disease: a clinico-pathological study of 100 cases. *J. Neurol. Neurosurg. Psychiatry* **55**, 181–184 (1992).
41. American Academy of Sleep Medicine (AASM). *International Classification of Sleep Disorders* 3rd edn. (ICSD-3). AASM International Classification of Sleep Disorders, 3rd ed, text revision (ICSD-3-TR) <https://aasm.org/clinical-resources/international-classification-sleep-disorders> (2023).
42. Hoehn, M. M. & Yahr, M. D. Parkinsonism: onset, progression and mortality. *Neurology* **17**, 427–442 (1967).
43. Goetz, C. G. et al. Movement Disorder Society-sponsored revision of the Unified Parkinson's Disease Rating Scale (MDS-UPDRS): scale presentation and clinimetric testing results. *Mov. Disord.* **23**, 2129–2170 (2008).
44. Folstein, M. F., Folstein, S. E. & McHugh, P. R. Mini-mental state. A practical method for grading the cognitive state of patients for the clinician. *J. Psychiatr. Res.* **12**, 189–198 (1975).
45. Nasreddine, Z. S. et al. The Montreal Cognitive Assessment, MoCA: a brief screening tool for mild cognitive impairment. *J. Am. Geriatr. Soc.* **53**, 695–699 (2005).
46. Beck, A. T., Steer, R. A. & Brown, G. Beck Depression Inventory-II. *PsycTESTS Dataset* <https://doi.org/10.1037/t00742-000> (2011).
47. Sletten, D. M., Suarez, G. A., Low, P. A., Mandrekar, J. & Singer, W. COMPASS 31: a refined and abbreviated Composite Autonomic Symptom Score. *Mayo Clin. Proc.* **87**, 1196–1201 (2012).
48. Stiasny-Kolster, K. et al. The REM sleep behavior disorder screening questionnaire—a new diagnostic instrument. *Mov. Disord.* **22**, 2386–2393 (2007).
49. Tomlinson, C. L. et al. Systematic review of levodopa dose equivalency reporting in Parkinson's disease. *Mov. Disord.* **25**, 2649–2653 (2010).
50. Chen H., Zhou Y., Liu Y., Zhang P. & Chen M. Network integration and protein structural binding analysis of neurodegeneration-related interactome. *Brief Bioinform.* **24**, <https://doi.org/10.1093/bib/bbad237> (2023).

Acknowledgements

T.B. was funded by the SEED4IP, the Ministry of Enterprises and Made in Italy (MIMIT), NADINE: JNK3 as a central and peripheral biomarker for synaptic dysfunction in neurodegenerative and psychiatric diseases, and by RECOGNIZED, the European Commission's Horizon 2020 research and

innovation program (No. 847749). G.M. received funds from the Swiss Parkinson Foundation Research Grant, the Synapsis Foundation Research Grant 2022-PI06, and the AFRI-EOC Research Support. Acknowledgment to the DisFeB Excellence Project, University of Milan, Italy. Open Access funding enabled and organized by T.B grants.

Author contributions

E.V.-acquisition, statistical analysis, interpretation of data, and drafted the manuscript, skin biopsy collection, immunofluorescence and immunofluorescence evaluation and analysis. M.G.B., L.B., F.P., S.R., S.M., M.M., G.K., I.B., G.B., S.G., A.K., S.H.-patient enrollment, data interpretation, and manuscript revision. G.M.-study conceptualization, data analysis and interpretation, study coordination, patients enrollment, clinical assessment, draft writing, and manuscript revision. A.G.-performed and optimized the JNK3 measurements, western blot, sample preparation and characterization; carried out SIMOA statistical analysis; interpreted the data; drafted and revised the manuscript. S.T. carried out the JNK3 assays, western blot, and sample preparation, contributed to data interpretation, and manuscript revision. V.B., L.P.-performed and controlled the SIMOA measurements; contributed to data validation. N.P.-performed data analysis, interpretation, and bioinformatics analysis; drafted and revised the manuscript; designed the figures. D.R.-led bioinformatics data analysis and interpretation; revised the manuscript. M.R. contributed to data interpretation and analysis; revised the manuscript. M.T.-led and supervised statistical analysis of the experimental results; contributed to manuscript revision. T.B. -conceived and directed the project; developed the main conceptual framework and outlined the study design; supervised all research activities, data analysis and interpretation; coordinated the writing process and wrote the manuscript.

Competing interests

The authors declare no competing interests.

Additional information

Supplementary information The online version contains supplementary material available at <https://doi.org/10.1038/s41531-025-01224-4>.

Correspondence and requests for materials should be addressed to Giorgia Melli or Tiziana Borsello.

Reprints and permissions information is available at <http://www.nature.com/reprints>

Publisher's note Springer Nature remains neutral with regard to jurisdictional claims in published maps and institutional affiliations.

Open Access This article is licensed under a Creative Commons Attribution-NonCommercial-NoDerivatives 4.0 International License, which permits any non-commercial use, sharing, distribution and reproduction in any medium or format, as long as you give appropriate credit to the original author(s) and the source, provide a link to the Creative Commons licence, and indicate if you modified the licensed material. You do not have permission under this licence to share adapted material derived from this article or parts of it. The images or other third party material in this article are included in the article's Creative Commons licence, unless indicated otherwise in a credit line to the material. If material is not included in the article's Creative Commons licence and your intended use is not permitted by statutory regulation or exceeds the permitted use, you will need to obtain permission directly from the copyright holder. To view a copy of this licence, visit <http://creativecommons.org/licenses/by-nc-nd/4.0/>.